PHYSICAL REVIEW C, VOLUME 63, 021307(R)

Excited states in ^{103}Sn: Neutron single-particle energies with respect to ^{100}Sn

C. Fahlander,[1] M. Palacz,[2] D. Rudolph,[1] D. Sohler,[3] J. Blomqvist,[4] J. Kownacki,[2] K. Lagergren,[4] L. O. Norlin,[4] J. Nyberg,[5] A. Algora,[6] C. Andreoiu,[1] G. de Angelis,[6] A. Ataç,[5] D. Bazzacco,[7] L. Berglund,[1] T. Bäck,[4] J. Cederkäll,[4] B. Cederwall,[4] Zs. Dombradi,[3] B. Fant,[8] E. Farnea,[9] A. Gadea,[6,9] M. Górska,[10] H. Grawe,[10] N. Hashimoto-Saitoh,[11] A. Johnson,[4] A. Kerek,[4] W. Klamra,[4] S. M. Lenzi,[7] A. Likar,[12] M. Lipoglavšek,[12] M. Moszyński,[13] D. R. Napoli,[6] C. Rossi-Alvarez,[7] H. A. Roth,[14] T. Saitoh,[11] D. Seweryniak,[15] Ö. Skeppstedt,[14] M. Weiszflog,[5] and M. Wolińska[2]

[1]*Department of Physics, Lund University, Lund, Sweden*
[2]*Heavy Ion Laboratory, University of Warsaw, Warsaw, Poland*
[3]*Institute for Nuclear Research, Debrecen, Hungary*
[4]*Royal Institute of Technology, Stockholm, Sweden*
[5]*Department of Neutron Research, Uppsala University, Uppsala, Sweden*
[6]*Laboratori Nazionali di Legnaro, Padova, Italy*
[7]*Dipartimento di Fisica and INFN, Sezione di Padova, Padova, Italy*
[8]*Department of Physics, Helsinki University, Helsinki, Finland*
[9]*Instituto de Fisica Corpuscular, Valencia, Spain*
[10]*GSI, Darmstadt, Germany*
[11]*Niels Bohr Institute, University of Copenhagen, Copenhagen, Denmark*
[12]*J. Stefan Institute, Ljubljana, Slovenia*
[13]*Sołtan Institute for Nuclear Studies, Świerk, Poland*
[14]*Chalmers University of Technology, Gothenburg, Sweden*
[15]*Argonne National Laboratory, Argonne, Illinois 60439*

(Received 26 May 2000; published 24 January 2001)

Gamma-ray lines from ^{103}Sn have been identified for the first time using EUROBALL and ancillary detectors. The level scheme of ^{103}Sn has been established by means of particle-gated $\gamma\gamma$ coincidences. The energy spacing between the $g_{7/2}$ and $d_{5/2}$ neutron single-particle orbitals is determined from the excited states in ^{103}Sn.

DOI: 10.1103/PhysRevC.63.021307 PACS number(s): 21.60.Cs, 23.20.Lv, 27.60.+j

^{100}Sn is the heaviest particle-bound doubly magic nucleus with $T_z=0$, i.e., with equal number of protons and neutrons. Nuclei in its vicinity provide a unique opportunity to study interactions of protons and neutrons in a many-body system close to the proton drip line with the two kinds of nucleons filling identical orbitals. Proton-neutron pairing suggested by theoretical investigations [1] is a unique phenomenon for such systems, and the influence of continuum states on bound levels may be studied [2], which is a vastly unknown aspect of nuclear structure. It was pointed out recently that there is an intimate relation between the pairing part of a realistic interaction, deduced by *G*-matrix many-body theory from *NN* phase shifts [3], and the physics of neutron stars mediated by this interaction [4].

Precise knowledge of single-particle energies (SPE) with respect to ^{100}Sn provides a stringent test of relativistic mean field [5] and Hartree-Fock [6] predictions. The neutron SPE could be inferred by studying excited states in ^{101}Sn. However, at present this extremely neutron deficient nucleus is not accessible for in-beam studies. The SPE have to be estimated from the comparison of known excited states with the results of shell-model calculations in more distant odd-*A* neighbors of ^{100}Sn, but the further away one moves from the doubly magic core the more hampered such estimates become because of uncertain two-body interactions of the valence nucleons. As long as studies of excited states in ^{101}Sn are not feasible, the best possible information on neutron SPE with respect to ^{100}Sn is provided by ^{103}Sn. Here we report on the first identification of its excited states.

The experiment was performed at Laboratori Nazionali di Legnaro in Italy using the reaction ^{58}Ni+^{54}Fe leading to the compound nucleus ^{112}Xe at a beam energy of 240 MeV. The ^{54}Fe target enriched to 99.915% and with a thickness of 1.4 mg/cm^2 was evaporated onto 13.0 mg/cm^2 of gold backing. The experiment suffered from buildup of oxygen on the target leading to reactions of ^{58}Ni on mainly ^{16}O. Therefore, the ^{54}Fe target was replaced with a fresh target after about half the experiment.

The experiment employed the EUROBALL [7] Ge detector array, which was equipped with 26 clover [8] and 15 cluster [9] composite Compton suppressed Ge detectors. EUROBALL was coupled to the 4π charged particle detection device ISIS [10], consisting of 40 silicon $\Delta E/E$ telescopes, and to the dedicated EUROBALL Neutron Wall [11], which consists of 50 liquid scintillator neutron detectors covering the forward 1π section of EUROBALL.

The trigger system required that at least one γ ray was detected in EUROBALL in coincidence with at least one hardware prediscriminated neutron in the neutron wall, or alternatively that 7 γ rays were detected in EUROBALL. The logical OR of the time aligned constant fraction signals from the neutron detectors was used as a time reference for all other signals.

In the off-line analysis a semiautomatic gain matching and shift correction procedure [12] was used. Alpha particles and protons registered in the ISIS Si ball were discriminated by setting limits on the energy deposited in the ΔE and E detectors. The resulting proton and α-particle detection efficiency was estimated to about 55% and 37%, respectively.

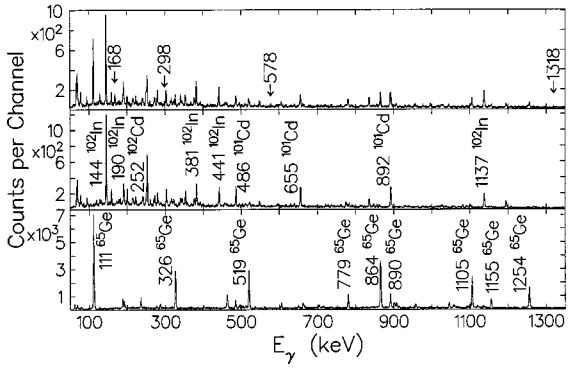

FIG. 1. Gamma-ray spectra obtained in the ^{58}Ni+^{54}Fe reaction: (a) $2\alpha 1n$ gated, (b) $2\alpha 1n1p$ gated, (c) cleaned ^{65}Ge spectrum from the reaction ^{58}Ni+^{12}C [14].

Both γ rays and neutrons were detected in the Neutron Wall detectors. They were distinguished by setting limits on two signals provided by each of the detectors: the time of flight (t_{tof}) between the target and the detector and the zero-cross-over time (t_{zco}). However, in a significant fraction of neutron events, the time reference was provided by a neutron itself, rather than a γ ray, resulting in $t_{tof}\approx 0$ for the neutron. This effect was especially important for low γ-ray multiplicity channels, as, e.g., the $2\alpha 1n$ channel [13], where about 70% of the neutrons were registered with $t_{tof}\approx 0$. For such events additional conditions on the time signals of the Ge and ISIS detectors had to be used. Altogether about 80% of the on-line discriminated neutrons passed the off-line discrimination conditions.

The ^{103}Sn nucleus is produced with the emission from the compound nucleus of two α particles and one neutron. A spectrum gated with the requirement that two α particles and one neutron were detected is shown in Fig. 1(a). This spectrum is dominated by γ-ray lines from ^{102}In, ^{101}Cd, and ^{65}Ge. The ^{102}In and ^{101}Cd nuclei are produced with the emission of one and two more protons, respectively. A spectrum gated by two α particles, one neutron, and one proton is shown in Fig. 1(b). Lines from ^{65}Ge, which arise from the $2\alpha 1n$ reaction on the ^{16}O target contamination, are not present in the $2\alpha 1p1n$ gated spectrum. This shows the high quality of the particle gating procedures. Nevertheless, with the contaminating lines as strong as in Fig. 1(a), a convincing way of discriminating between lines from reactions on ^{54}Fe and the ^{16}O contamination is needed. For this purpose, we show in Fig. 1(c) a cleaned ^{65}Ge spectrum obtained in the reaction ^{58}Ni+^{12}C at a bombarding energy of 261 MeV [14].

The search for γ-ray lines from ^{103}Sn was performed by a careful analysis of the spectra shown in Figs. 1(a) and 1(b). Candidates are γ-ray lines which are present in the $2\alpha 1n$-gated spectrum, but not in the $2\alpha 1n1p$-gated spectrum. In addition they should not be present in the spectrum shown in Fig. 1(c). The lines at 168, 298, 578, and 1318 keV fulfil these conditions. The parts of the spectra in Fig. 1 relevant to these four transitions are displayed in Fig. 2 in more detail. The 298, 578, and 1318 keV lines are not observed in other particle-gated spectra, whereas the 168 keV

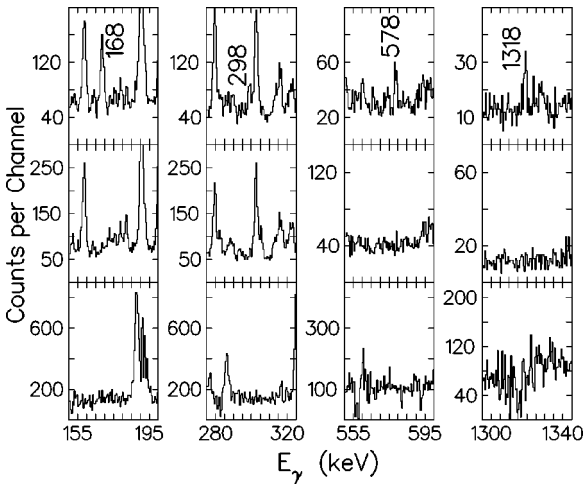

FIG. 2. Parts of interest of the γ-ray spectra of Fig. 1.

line forms a small peak on a very large background in the $1\alpha 1n$-gated spectrum, but the intensity of the 168 keV peak in that spectrum is in agreement with the assumption that it belongs to the $2\alpha 1n$ reaction channel. Also, the contamination related lines from oxygen building up on the target became stronger with time, which was not the case with, e.g., the 168 keV line.

In the next step a prompt $\gamma\gamma$ coincidence matrix was created with the condition that two α particles and one neutron were detected. Spectra in coincidence with the 168, 298, 578, and 1318 keV γ rays are shown Fig. 3, together with local background spectra.

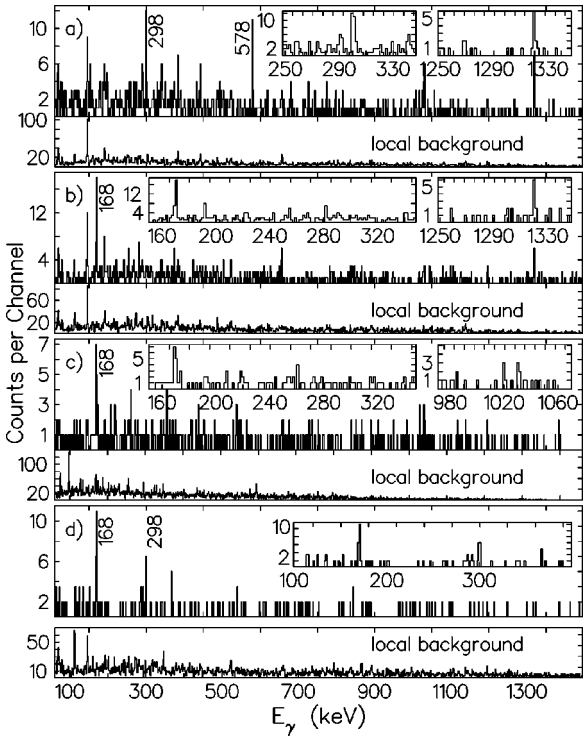

FIG. 3. $2\alpha 1n$-gated γ-ray spectra in coincidence with the 168 (a), 298 (b), 578 (c), and 1318 keV (d) transitions. Expanded parts of the three spectra are presented in the insets.

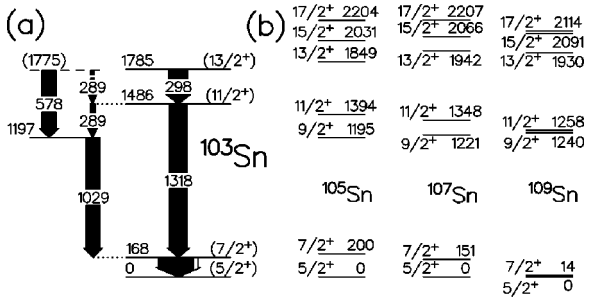

FIG. 4. Level scheme of ^{103}Sn (a) and the systematics of odd-A neutron deficient Sn isotopes (b). The widths of the arrows are proportional to the γ-ray intensities. The white part of the 168 keV arrow represents internal conversion.

Based on these results we propose the level scheme of ^{103}Sn shown in Fig. 4(a). Although the statistics in the coincidence spectra is small they clearly show that the γ-ray lines 168, 298, and 1318 keV are in mutual coincidence. The 578 keV line is in coincidence with the 168 and 1029 keV lines. However, due to the low statistics it is not possible to make a firm placement of the 578 keV transition. None of these γ-ray lines is in coincidence with any of the strong lines belonging to other nuclei seen in the $2\alpha 1n$ gated spectrum. The 289 keV line matches the energy difference between the 1486 and 1197 keV levels as well as between the 1775 and 1486 keV levels, but it is not possible to establish whether the 289 keV line is a doublet or not. The existence of the 289 and 1029 keV lines supports the placement of the 1197 keV level. However, evidence of a possible 1197 keV transition to the ground state is uncertain due to the existence of strong lines of similar energy in several other strongly populated nuclei.

We conclude that the observed γ-ray lines belong to the ^{103}Sn nucleus. They are listed in Table I. The cross section for the production of ^{103}Sn relative to the total fusion evaporation cross section is estimated to be less than 2×10^{-5}, which corresponds to an absolute cross section of about 10 μb.

The ground state spin and parity of ^{103}Sn are not known. However, based on a systematic comparison with the other odd-A neutron deficient Sn isotopes [Fig. 4(b)], we propose spin and parity $(5/2^+)$ for the ground state of ^{103}Sn.

Despite the low statistics limited information on angular properties of the γ rays were obtained from the data. The ratios $R=I_{\theta_1}/I_{\theta_2}$ of γ-ray intensities measured at two different angles with respect to the beam axis were determined (see Table I), where I_{θ_1} corresponds to the intensity measured in the cluster detectors at angles 123° and 164° and I_{θ_2} to the intensity in the clover detectors at 72° and 107°. Based on values obtained for transitions of known multipolarity we expect $R=0.60$ and $R=0.97$ for stretched dipole and quadrupole transitions, respectively. We thus assign a spin difference of $\Delta I=1$ to the 168 and 298 keV transitions. The R value for the 1318 keV transition has a large error, but it is in agreement with a spin difference of $\Delta I=2$. The 1197 keV level is likely the $9/2^+$ state suggested by systematics.

TABLE I. Energy (E_γ), relative intensity (I_γ), and angular distribution ratio (R) of γ-ray transitions in ^{103}Sn.

E_γ (keV)	I_γ	R
168.0±0.1	100±7	0.62±0.07
289.0±0.2 [a]	35±7	
298.4±0.1	54±8	0.57±0.12
578.2±0.2	41±7	0.99±0.32
1029.0±1.0 [b]	40±23	
1318.2±0.3	50±9	1.07±0.30

[a]Possibly a doublet.

[b]Intensity estimated from coincidence spectra.

Experimental properties (mainly excitation energies and electromagnetic transition rates) of low-lying states in light Sn isotopes can be compared with results from shell-model calculations with a truncated single-particle basis $1g_{7/2}$, $2d_{5/2}$, $2d_{3/2}$, $3s_{1/2}$, $1h_{11/2}$ for the valence neutrons [3,15–18]. Such calculations are hampered by the lack of experimental values for the SPE in ^{101}Sn. Furthermore, the effective interaction matrix elements derived from the bare two-nucleon interaction [3,15] are known in other regions to be burdened by significant errors, which limits the full exploitation of the powerful shell-model theory. Alternatively, one could extract empirical effective interaction matrix elements if complete data were available in ^{102}Sn, but this is not possible since only the lowest 0^+, 2^+, 4^+, and 6^+ levels are known in this nucleus [19].

As a consequence of these problems one may instead be led to exploit the richer experimental information available for Sn isotopes with several neutrons added to ^{100}Sn [20,21], or the $N=51$ isotones of ^{101}Sn [16,22,23], by varying the input parameters, i.e., the single-particle energies and two-body matrix elements, in the shell model code to obtain a good fit to the observed excitation energies and transition rates in these heavier Sn isotopes. The difficulty with such an approach derives from the large number of parameters, and from the highly nonlinear dependence of output on input, giving rise to ambiguities in the fitting procedure. These ambiguities can be relieved by constraints on the parameters put by even sparse data from nuclei with fewer valence neutrons. The $1g_{7/2}$ and $2d_{5/2}$ orbitals are of particular interest. The former determine the $l=4$ spin-orbit splitting, while the $2d_{5/2}$ level is part of the strong $g_{9/2}^{-1}\ d_{5/2}\ 2^+$ core excitation, as is known from ^{56}Ni one major shell lower [24].

From this point of view the data obtained in this work gives important information. The energy $E(7/2^+,{}^{103}\mathrm{Sn})=168$ keV constrains the single-particle energy difference $\epsilon(1g_{7/2})-\epsilon(2d_{5/2})$ more effectively than was previously possible from the $7/2^+$ energies in ^{105}Sn and ^{107}Sn and from the $N=51$ isotones [16,22,23]. A shell-model calculation using the matrix elements [3] derived from the Bonn-A potential, with some empirical corrections to improve the overall fit to $^{102-114}$Sn, gives the predicted value $\epsilon(1g_{7/2})-\epsilon(2d_{5/2})=0.11(4)$ MeV. The error represents an estimate of the uncertainty related to variations of the effective interaction.

The energies of the $3s_{1/2}$, $2d_{3/2}$, and $1h_{11/2}$ single-particle states, completing the 50–82 major neutron shell, are

not well constrained by the present ^{103}Sn data. However, by making full shell model calculations in the $d_{5/2}$, $g_{7/2}$, $s_{1/2}$, $d_{3/2}$, $h_{11/2}$ basis, and by fitting to experimental one-quasiparticle energies in heavier odd-*A* Sn isotopes up to ^{113}Sn, these SPE in ^{101}Sn are estimated to be $\epsilon(3s_{1/2}) = 1.6(2)$ MeV, $\epsilon(2d_{3/2}) = 2.0(2)$ MeV, and $\epsilon(1h_{11/2}) = 2.3(2)$ MeV. The gap between the neutron shells $2d_{5/2}$, $1g_{7/2}$ and $s_{1/2}$, $d_{3/2}$, $h_{11/2}$ is somewhat smaller than the gap between the corresponding proton shells, and therefore gives rise to a smaller irregularity in the mass surfaces at $N=64$ than at $Z=64$ [25].

The shell-model calculations for Sn isotopes up to ^{114}Sn, using phenomenological SPE and effective interactions for the five neutron shells between 50 and 82, give in general satisfactory results in comparison with experimental energies. However, for a few levels in nuclei close to ^{100}Sn there are striking disagreements between calculated and experimental energies. An example of this is the spacing between the yrast 4^+ and 6^+ levels in ^{104}Sn, which is typically underpredicted by about 200 keV. In similar calculations for the lead isotopes $^{202-206}$Pb all disagreements are smaller than 100 keV for states which do not for the main part involve particle-hole excitations of the ^{208}Pb core. This may indicate that core excitations across $N=Z=50$ in ^{100}Sn are more strongly coupled to specific neutron states than is the case for core excitations across $Z=82$, $N=126$ in the Pb region. To shed more light on this problem it would be interesting to locate the $15/2^+$ and $17/2^+$ levels in ^{103}Sn, which are predicted to complete the yrast line before a gap of about 2 MeV opens up to negative parity levels $19/2^-$ and $21/2^-$.

In summary the results of the present experiment allow the most accurate estimate to date for the relative SPE of the neutron $d_{5/2}$ and $g_{7/2}$ orbitals with respect to ^{100}Sn. A complete set of SPE in the $d_{5/2}$, $g_{7/2}$, $s_{1/2}$, $d_{3/2}$, $h_{11/2}$ model space will be subject to future experiments. This includes investigation of the role of the low-lying 2^+ and 3^- core excitations in high-spin states.

This research was supported by the Swedish Natural Science Research Council and the European Commission (EC) TMR/LSF Contract No. ERBFMGECT980110. E.F. and A.G. were supported by the EC under Contract Nos. ERBFMBICT983126 and ERBCHBGCT940713, respectively. One of the authors (D. Sohler) was supported by the Göran Gustafsson Foundation OTKA(30497).

[1] W. Nazarewicz *et al.*, Phys. Scr. **T56**, 9 (1995).
[2] J. Dobaczewski *et al.*, Phys. Rev. C **53**, 2809 (1996).
[3] M. Hjorth-Jensen *et al.*, Phys. Rep. **261**, 125 (1995).
[4] H. Heiselberg and M. Hjorth-Jensen, Phys. Rep. **328**, 237 (2000).
[5] K. Rutz *et al.*, Nucl. Phys. **A634**, 67 (1998).
[6] B. A. Brown, Phys. Rev. C **58**, 220 (1998).
[7] *EUROBALL III, A European γ-ray Facility*, edited by J. Gerl and R. M. Lieder (GSI, Darmstadt, 1992).
[8] G. Duchêne *et al.*, Nucl. Instrum. Methods Phys. Res. A **432**, 90 (1999).
[9] J. Eberth *et al.*, Nucl. Instrum. Methods Phys. Res. A **369**, 135 (1996).
[10] E. Farnea *et al.*, Nucl. Instrum. Methods Phys. Res. A **400**, 87 (1997).
[11] Ö. Skeppstedt *et al.*, Nucl. Instrum. Methods Phys. Res. A **421**, 531 (1999).
[12] M. Palacz *et al.*, Nucl. Instrum. Methods Phys. Res. A **383**, 473 (1996).
[13] M. Wolinska *et al.* (to be published).
[14] D. Sohler *et al.*, Nucl. Phys. **A644**, 141 (1998).
[15] F. Andreozzi *et al.*, Phys. Rev. C **54**, 1636 (1996).
[16] H. Grawe *et al.*, Phys. Scr. **T56**, 71 (1995).
[17] R. Schubart *et al.*, Z. Phys. A **352**, 373 (1995).
[18] B. A. Brown and K. Rykaczewski, Phys. Rev. C **50**, R2270 (1994).
[19] M. Lipoglavšek *et al.*, Phys. Lett. B **440**, 246 (1998).
[20] M. Górska *et al.*, Phys. Rev. C **58**, 108 (1998).
[21] S. Juutinen *et al.*, Nucl. Phys. **A617**, 74 (1997).
[22] M. Górska *et al.*, in *The Physics of Electronic and Atomic Collisions*, edited by Torkild Andersen, Bent Fastrup, Finn Folkmann, Helge Knudsen, and N. Andersen, AIP Conf. Proc. No. 295 (AIP, New York, 1993), p. 217.
[23] H. Grawe *et al.*, Proceedings of ''The beta decay, from weak interaction to nuclear structure,'' IReS Strasbourg, 1999, edited by Ph. Dessagne, A. Michalon, and Ch. Miehé, p. 211.
[24] G. Kraus *et al.*, Phys. Rev. Lett. **73**, 1773 (1994).
[25] J. Blomqvist *et al.*, Z. Phys. A **312**, 27 (1983).